Binding of Small Basic Peptides to Membranes Containing Acidic Lipids: Theoretical Models and Experimental Results

Nir Ben-Tal,* Barry Honig,* Robert M. Peitzsch,# Gennady Denisov,# and Stuart McLaughlin#
*Department of Biochemistry and Molecular Biophysics and Center for Biomolecular Simulations, Columbia University, New York, New York 10032; and #Department of Physiology and Biophysics, Health Sciences Center, SUNY Stony Brook, Stony Brook, New York 11794-8661 USA

ABSTRACT We measured directly the binding of Lys_3, Lys_5, and Lys_7 to vesicles containing acidic phospholipids. When the vesicles contain 33% acidic lipids and the aqueous solution contains 100 mM monovalent salt, the standard Gibbs free energy for the binding of these peptides is 3, 5, and 7 kcal/mol, respectively. The binding energies decrease as the mol% of acidic lipids in the membrane decreases and/or as the salt concentration increases. Several lines of evidence suggest that these hydrophilic peptides do not penetrate the polar headgroup region of the membrane and that the binding is mainly due to electrostatic interactions. To calculate the binding energies from classical electrostatics, we applied the nonlinear Poisson-Boltzmann equation to atomic models of the phospholipid bilayers and the basic peptides in aqueous solution. The electrostatic free energy of interaction, which arises from both a long-range coulombic attraction between the positively charged peptide and the negatively charged lipid bilayer, and a short-range Born or image charge repulsion, is a minimum when ~2.5 Å (i.e., one layer of water) exists between the van der Waals surfaces of the peptide and the lipid bilayer. The calculated molar association constants, K, agree well with the measured values: K is typically about 10-fold smaller than the experimental value (i.e., a difference of about 1.5 kcal/mol in the free energy of binding). The predicted dependence of K (or the binding free energies) on the ionic strength of the solution, the mol% of acidic lipids in the membrane, and the number of basic residues in the peptide agree very well with the experimental measurements. These calculations are relevant to the membrane binding of a number of important proteins that contain clusters of basic residues.

INTRODUCTION

Many proteins have a cluster of basic residues that facilitate their adsorption to membranes—the basic residues interact with acidic lipids. These electrostatic interactions often occur in conjunction with the hydrophobic penetration of a myristoyl or farnesyl group on the proteins into the interior of the membrane. Examples of myristoylated proteins that use this mechanism include Src (Resh, 1993, 1994; Buser et al., 1994; Sigal et al., 1994), MARCKS (Aderem, 1992; Blackshear, 1993; McLaughlin and Aderem, 1995), and the HIV matrix protein (Zhou et al., 1994; Massiah et al., 1994); an example of a farnesylated protein that uses this mechanism is K-ras (Hancock et al., 1990; Cadwallader et al., 1994). The binding of MARCKS to membranes can be reversed by PKC phosphorylation of serine residues within the cluster, which places negatively charged phosphate groups within the cluster, weakens the electrostatic interaction, and allows the protein to translocate to the cytoplasm because the myristate group does not provide sufficient hydrophobic energy to anchor the protein (McLaughlin and Aderem, 1995). The main objective of this report is to provide a theoretical description of the electrostatic interaction of basic peptides with membranes containing acidic lipids.

Short hydrophilic peptides containing basic residues bind to membranes containing acidic lipids (Dufourcq et al., 1981; de Kruijff et al., 1985; Roux et al., 1988; de Kroon et al., 1990, 1991; Kim et al., 1991; Thorgeirsson et al., 1995). A theoretical model that combines the Gouy-Chapman-Stern theory of the electrostatic potential adjacent to a charged membrane, the Boltzmann relation, and mass action equations accounts qualitatively for the binding data (Kim et al., 1991; Thorgeirsson et al., 1995). Two groups have reported more detailed theoretical studies of the electrostatic interactions of proteins with surfaces: Yoon and Lenhoff (1992) studied the interaction of positively charged ribonuclease A with a negatively charged surface, and Roush et al. (1994) studied the interaction of negatively charged rat cytochrome b_5 with a positively charged surface. The electrostatic energy of interaction of the proteins and the surfaces was analyzed using continuum solvent models. (For reviews of continuum solvent models and their biological and chemical applications, see Davis and McCammon (1990), Honig et al. (1993), Sharp (1994), and Honig and Nicholls (1995).) Roth and Lenhoff (1993) extended the method to account for van der Waals (dispersion) interactions between the adsorbed protein and the surface, and they calculated the binding constant of the protein to the surface from the energy of interaction.

We report here a systematic study of the binding of three basic peptides, $(Lys)_3$, $(Lys)_5$, and $(Lys)_7$, to phospholipid vesicles under conditions where the peptide concentration is

Received for publication 9 February 1996 and in final form 26 April 1996.

Address reprint requests to Dr. Stuart G. McLaughlin, Department of Physiology and Biophysics, SUNY Health Science Center–Stony Brook, Stony Brook, NY 11794-8661. Tel.: 516-444-3615; Fax: 516-444-3432; E-mail: smcl@epo.som.sunysb.edu.

Dr. Denison's permanent address is Institute of Mathematical Problems of Biology, Academy of Sciences of Russia, Pushchino, Moscow Region 142292, Russia.

0006-3495/96/08/561/15 $2.00

sufficiently low that peptide-peptide interactions are vanishingly small. The available evidence suggests that the binding of the peptides is due mainly to electrostatic interactions. 1) Small basic peptides like $(Lys)_5$ do not bind to membranes formed from electrically neutral lipids like phosphatydylcholine (PC) (Mosior and McLaughlin, 1992a). 2) Binding increases as the mol% of acidic lipids in membrane increases (Mosior and McLaughlin, 1992b; see also below). 3) Binding decreases as the salt concentration increases (Mosior and McLaughlin, 1992b; see also below). 4) The binding is independent of the chemical nature of the acidic lipids or the basic residues (Kim et al., 1991; Mosior and McLaughlin, 1992a). 5) Peptides like $(Lys)_5$ bind outside the envelope of the polar headgroup, as indicated by NMR (Roux et al., 1988), high-pressure fluorescence (Montich et al., 1993), and monolayer surface pressure (Kim et al., 1991; see also below) measurements.

We present two theoretical models, based on classical electrostatics, for calculating the binding constant of the positively charged peptides to the negatively charged membranes. Following the approach outlined in standard electrochemistry texts (e.g., Bockris and Kahn, 1993) and described in detail below (see Fig. 1), we calculated the binding constant by evaluating the Gibbs surface excess of the peptide adjacent to the membrane. The peptide concentration at any distance from the membrane surface depends in a Boltzmann manner on its electrostatic free energy of interaction with the membrane, which is calculated by solving the nonlinear Poisson-Boltzmann equation.

In the first model, the peptide is represented by a point charge and the membrane by a uniformly charged surface. This simplified geometry allows one to obtain an analytical expression for the energy of interaction at each peptide-membrane distance in terms of the Gouy-Chapman-Stern theory. In the second model both the peptide and the membrane (Peitzsch et al., 1995) are represented in atomic detail. The reciprocal effects of the peptide and the membrane on each other's electrostatic potentials, which were ignored in the first model, are taken into account and give rise to a Born repulsion between the peptide and the membrane at a short distance. The short-range repulsion, when added to the long-range coulombic attraction between the oppositely charged membrane and peptide, yields a minimum in the electrostatic free energy of interaction between the membrane and the peptide. We compare the binding constants predicted by the two different theoretical models with the experimental results.

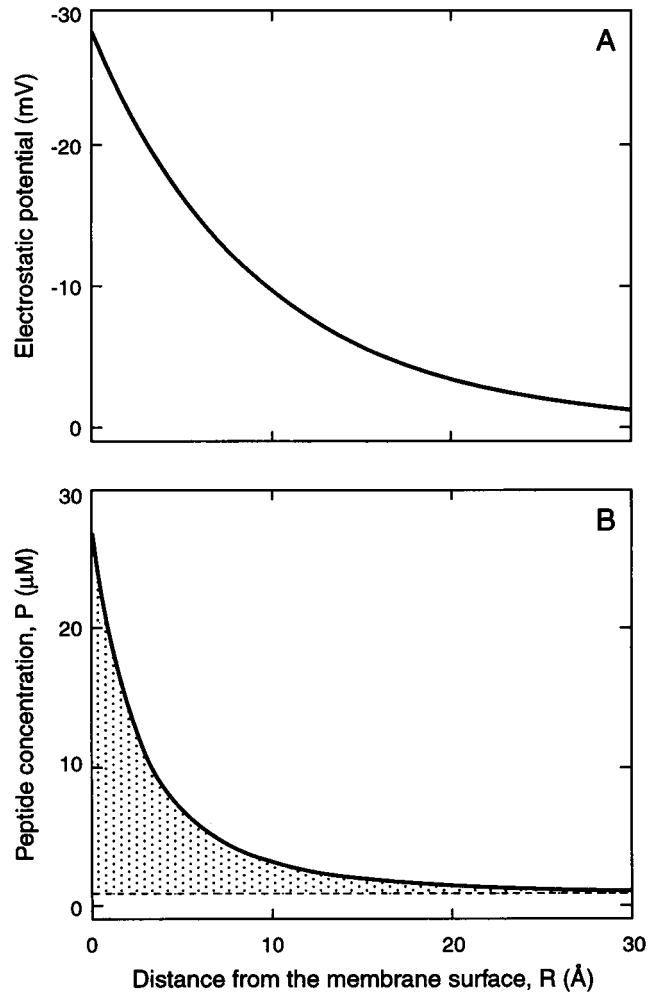

FIGURE 1 Sketch illustrating the concept of the Gibbs surface excess of peptide defined in Eq. 5. (*A*) In the primitive model the membrane is represented as a plane with a uniform surface charge density, and the electrostatic potential in the aqueous phase, $\phi(R)$, is described by Gouy-Chapman-Stern theory (Eqs. 12 and 13). The charge density we used for this figure corresponds to a 9:1 PC:PG membrane in 100 mM KCl. (*B*) The concentration of the *Z*-valent peptide a distance R from the membrane, $[P(R)] = [P(\infty)]\exp(-Z\phi(R))$, is calculated from the potential illustrated in *A* with $Z = 3$, corresponding to trilysine, and $[P(\infty)] = 10^{-6}$ M. The Gibbs surface excess is defined as the integral of $[P(R)] - [P(\infty)]$ over distance. This quantity, the stippled area in the figure, may be considered the number of trilysine peptides "adsorbed" to a unit area of membrane.

MATERIALS AND METHODS

Materials

The lipids 1-palmitoyl-2-oleoyl-*sn*-glycero-3-phosphocholine (PC) and 1-palmitoyl-2-oleoyl-*sn*-glycero-3-phosphoglycerol (PG) were purchased from Avanti Polar Lipids (Birmingham, AL). 1,2-Di[1-^{14}C]oleoyl-L-3-phosphocholine ([^{14}C]PC) was purchased from Amersham (Arlington Heights, IL). The peptides KKKKKKK, KKKKK, and KKK were synthesized by Multiple Peptides Systems (San Diego, CA) and were >95% pure, as determined by analytical high-performance liquid chromatography and mass spectrographic analyses.

Methods

Preparation of vesicles

Concentrations of PC and PG in $CHCl_3$ were measured on a Cahn electrobalance, a method that gives the same results as phosphate analysis (Kim et al., 1991; Peitzsch and McLaughlin, 1993). A mixture of lipids in a $CHCl_3$ solution was dried in a rotary evaporator under vacuum and resuspended in a sucrose solution (typically 176 mM sucrose, 1 mM 3-(*N*-morpholino)propanesulfonic acid (MOPS), pH 7.0). Large unilamellar vesicles (LUVs) were produced from the above lipid dispersions by the

method of Hope et al. (1985). In brief, the mixture was taken through five cycles of freezing (liquid N_2) and thawing (40°C water bath) followed by 10 cycles of extrusion through a stack of two polycarbonate filters (0.1-μm diameter pore size) in a Lipex biomembranes extruder (Vancouver, BC, Canada). Vesicles of this size are unilamellar (Mui et al., 1993). The sucrose solution on the outside of the vesicles was removed by dilution of the LUV solution to an isosmotic salt solution (typically 100 mM KCl, 1 mM MOPS, pH 7.0) and centrifugation (1 h, 100,000 × g, 25°C; for details see Rebecchi et al., 1992, and Buser et al., 1994). The supernatant was discarded and the resuspended pellet was used for the binding measurements. The incorporation of trace amounts of [^{14}C]PC into the lipid mixture allowed us to monitor the lipid concentration throughout the binding measurements.

Binding measurements

Peptides were mixed with sucrose-loaded LUVs under conditions where [peptide] ≪ [lipid], so the peptide did not bind a significant fraction of the acidic lipid in the vesicles. The mixture was equilibrated for 15 min at room temperature (22°C) and then separated by centrifugation (1 h, 100,000 × g, 25°C). Ninety percent of the supernatant was retrieved immediately, and the concentrations of peptide in the supernatant and pellet were measured by a fluorescamine assay as described by Buser et al. (1994). Calculations of the percentage of bound peptide were corrected for the 1–5% lipid that remained in the supernatant.

For technical reasons we used the acidic lipid PG rather than PS for these binding measurements (the breakdown of a small fraction of PS produces amines that are detected by the fluorescamine technique). Most of our theoretical calculations were carried out with the acidic lipid PS, because this is the major acidic lipid in a mammalian biological membrane. Previous electrophoretic mobility measurements showed that trilysine and pentalysine bind with identical affinities to vesicles formed from either PG or PS (see figure 1 of Kim et al., 1991).

Monolayer measurements

We used an apparatus designed by Fromherz (1975) (purchased from Mayer Feintechnik, Göttingen, Germany) to show that when Lys_5 molecules adsorb to lipid monolayers they do not penetrate significantly into the monolayer. This apparatus monitors the surface pressure of the monolayer by means of a Wilhemy plate and has a feedback circuit that increases the area of the monolayer to maintain a constant surface pressure as any adsorbing solute penetrates into the monolayer. Adsorption of molecules that would be expected to penetrate the monolayer, such as dibucaine (Seelig, 1987), signal peptides (Tamm, 1991), substance P antagonists (Seelig, 1992), myristic acid, and short-chain phospholipids (Boguslavsky et al., 1994), produces an increase in area. The addition of 4×10^{-5} or 8×10^{-5} M Lys_5 to a monolayer formed from 2:1 PC:PG or PC:PS over a solution containing 100 mM KCl, 1 mM MOPS (pH 7) does not increase the surface pressure (π = 30 mN/m) at constant area or the area at constant surface pressure (π = 20, 30 mN/m), demonstrating that Lys_5 does not penetrate the monolayer upon adsorption.

Extracting binding constants and binding energies from experimental measurements

The binding of peptides to lipid bilayers can be described in terms of a molar partition coefficient, K, without making assumptions about the adsorption mechanism (see equation 1 of Peitzsch and McLaughlin, 1993). K is the proportionality factor between the mole fraction of peptide bound to the membrane, χ, and the molar concentration of peptide in the bulk aqueous phase, [P]. Under our experimental conditions, the molar concentration of lipid accessible to the peptide, [L], is much greater than the molar concentration of peptide bound to the membrane, $[P]_m$, so $\chi \approx [P]_m/[L]$ and

$$[P]_m = K[P][L]. \tag{1}$$

Hydrophilic basic peptides bind only to the outer surface of LUVs; hence $[L] = [L]_{tot}/2$, where $[L]_{tot}$ is the total molar concentration of lipid in the solution.

Equation 1 has the same form as the limiting version of a mass-action equation which assumes (incorrectly) that the peptide forms a 1:1 complex with a lipid. Thus K may be regarded as an apparent association constant. For our experiments we need consider only the limiting form of the equation (i.e., the Henry limiting law): because the peptide concentration is low, binding depends linearly on the concentration of peptide, the free lipid concentration is approximately equal to the total lipid concentration, and there is no significant interaction between the adsorbed peptides.

The total concentration of peptides in the solution, $[P]_{tot}$, is the sum of bound and free peptides:

$$[P] + [P]_m = [P]_{tot} \tag{2}$$

Substituting Eq. 2 in Eq. 1, one obtains

$$\frac{[P]_m}{[P]_{tot}} = \frac{K[L]}{1 + K[L]} \tag{3}$$

We determine the value of K by measuring the fraction of bound peptide, $[P]_m/[P]_{tot}$, as a function of [L]. We plot $[P]_m/[P]_{tot}$ versus [L] and obtain the value of K from a least-squares fit of Eq. 3 to the data; note that when $[P]_m/[P]_{tot} = 1/2$, $K = 1/[L]$.

If the peptide formed a 1:1 complex with a lipid, the association constant K would be related to the standard Gibbs free energy by

$$\Delta G^\circ = -Nk_BT \ln(K), \tag{4}$$

where N is Avogadro's number, k_B is Boltzmann's constant, and T is the temperature. We use Eq. 4 as a formalism to convert the experimentally determined molar partition coefficient K into energy units and refer below to ΔG^0 as the experimentally determined standard Gibbs free energy, or simply the binding free energy.

THEORETICAL MODELS

We calculate the binding energies of peptides to membranes using two different models. In the first we represent the peptide as a point and the membrane as a plane with the surface charge smeared uniformly. In the second we describe the peptide and the membrane in atomic detail. Because both the Debye length and the dimensions of the peptides are much smaller than the radius of the vesicles, we can assume the peptides interact with a planar surface. Because the peptides do not interact with each other, we studied the binding of a single peptide to the surface.

We assume the binding is purely electrostatic in nature. The negatively charged membrane concentrates the positively charged peptide in the aqueous diffuse double layer adjacent to the surface. We calculated the Gibbs surface excess, Γ, of the peptide to compare with our binding measurements. Γ is defined as (e.g., Bockris and Kahn, 1993)

$$\Gamma = C \int_0^\infty dR([P(R)] - [P(\infty)]), \tag{5}$$

where $[P(R)]$ is the peptide concentration at a distance R from the surface (R is the distance in Å between the van der Waals surfaces of the peptide and the membrane), Γ represents the number of moles of peptide "adsorbed" (through

nonspecific electrostatic interactions) to a unit area of surface in mol/dm^2 (see Fig. 1 *B*), and $C = 10^{-9}$ dm/Å is a units conversion factor.

By multiplying Γ by the area of the vesicles accessible to the peptides (i.e., the total area of the outer surfaces of the large unilamellar vesicles), A (in dm^2), and dividing by the volume of the solution, V (in dm^3), we obtain the total concentration of membrane-bound peptide in the solution, $[P]_m$. In other words,

$$[P]_m = \frac{A\Gamma}{V} \tag{6}$$

If the average free energy change that occurs when the peptide moves from the bulk aqueous solution at ∞ to a distance R is $\Delta W(R)$, then the concentration of peptides at a distance R, $[P(R)]$, is given by the Boltzmann relation

$$[P(R)] = [P(\infty)]\exp(-\beta\Delta W(R)), \tag{7}$$

where $\beta = (k_B T)^{-1}$. We assume that $\Delta W(R)$ arises only from electrostatic work and that we can calculate this energy using the (nonlinear) Poisson-Boltzmann equation. The calculation of $\Delta W(R)$ is trivial in model 1 but requires extensive calculations in the more realistic model 2.

Combining Eqs. 5, 6, and 7 we get

$$[P]_m = [P(\infty)]\frac{CA}{V}\int_0^\infty dR(\exp(-\beta\Delta W(R)) - 1). \tag{8}$$

Equation 8 represents the integral we must evaluate to calculate the apparent association constant of the peptide with the membrane. It is valid for all values of lipid concentration, or equivalently, all values of A/V. In particular, it is valid for $K[L] \ll 1$ in Eq. 3. In this limit $[P]_{tot} = [P(\infty)]$, such that Eq. 3 becomes

$$[P]_m = K[P(\infty)]\,[L]. \tag{9}$$

Note that by definition,

$$[L] = \frac{A}{A_L N V} \tag{10}$$

where A is the area of lipid available to the peptide, A_L is the area occupied by one lipid in the bilayer (68 Å^2 = 68 × 10^{-18} dm^2), and V is the volume of the solution. Combining Eqs. 8, 9, and 10, we obtain an expression for the binding constant as a function of the average free energy of the peptide a distance R from the membrane:

$$K = CA_L N\int_0^\infty dR(\exp(-\beta\Delta W(R)) - 1). \tag{11}$$

Equation 11 allows us to calculate a value of K that can be compared with our experimental value.

Model 1

We treat the system in the spirit of Gouy-Chapman theory (e.g., Aveyard and Haydon, 1973). Specifically, we assume the membrane is a plane with a uniform surface charge density. Monovalent ions (e.g., K^+, Cl^-) and the peptides are treated as points, and we neglect the effect of the peptide on the electric field. In addition, we apply a Stern correction to describe the adsorption of the monovalent cation K^+ to the acidic lipids. The Gouy-Chapman-Stern theory has been shown to accurately describe the electrostatic potential in the aqueous phase adjacent to a membrane (McLaughlin, 1989).

Gouy-Chapman theory describes how the electrostatic potential, $\phi(R)$ (in units of $k_B T/e$, where e is electron charge), depends on the distance from the surface, R:

$$\phi(R) = 2\ln\frac{1 + \tanh(\phi(0)/4)\exp(-\kappa R)}{1 - \tanh(\phi(0)/4)\exp(-\kappa R)} \tag{12}$$

where $\kappa = [(2\beta e^2 c^b)/(\epsilon_0\epsilon_r)]^{1/2}$ (c^b is the number of monovalent ions per unit volume in bulk, ϵ_0 is the permittivity in vacuum, and ϵ_r is the dielectric constant of water) is the Debye-Hückel parameter (e.g., κ^{-1} = 9.6 Å when the aqueous solution contains 100 mM monovalent ions at 25°C). The electrostatic potential at the surface, $\phi(0)$, is determined from the Gouy-Chapman-Stern equation

$$\sinh\left(\frac{\phi(0)}{2}\right) = (8Nk_B T\epsilon_0\epsilon_r[K^+])^{-1/2} \times \frac{\sigma_0}{1 + K_{KL}[K^+]\exp(-\phi(0))} \tag{13}$$

where σ_0 is the surface charge density in the absence of K^+ binding, and $[K^+]$ is the molar concentration of potassium ions in bulk. We deduced the value of the association constant of K^+ ions with the acidic lipids, $K_{KL} = 0.3\ M^{-1}$, that is appropriate for our experimental conditions from the zeta potential measurements of Kim et al. (1991). (The zeta potential is the potential at the hydrodynamic plane of shear, which is about 2 Å from the surface of the membrane in a 0.1 M monovalent salt solution (McLaughlin, 1989).) The Gouy-Chapman-Stern theory with this K_{KL} showed an excellent fit to the experimentally determined zeta potential measurements as a function of the mol% of acidic lipids.

Fig. 1 *A* illustrates the potential adjacent to a 9:1 PC:PS membrane predicted by this theory. The potential falls approximately exponentially with the distance from the surface (note from Eq. 12 that $\phi(R) \simeq \phi(0)\exp(-\kappa R)$ for small potentials) and the Debye length, κ^{-1}, is about 10 Å in this 100 mM monovalent salt solution.

The concentration of Z-valent peptide a distance R from the surface is calculated from the Boltzmann relation, Eq. 7, assuming that

$$\beta\Delta W(R) = Z\phi(R). \tag{14}$$

The Gibbs surface excess, as defined in Eq. 5, is illustrated by the stippled region in Fig. 1 *B*.

Model 2: atomic representation

We also carried out calculations using detailed atomic models of peptides and lipid bilayers. The free energy of binding of a peptide to a lipid bilayer was calculated in five stages described in detail in the subsections below:

1. The peptide was placed at a given distance from and orientation to the membrane (i.e., configuration) and mapped onto a cubic lattice.
2. The Poisson-Boltzmann equation (Eq. 21) was solved for the electrostatic potential at each lattice point for a particular configuration.
3. The electrostatic free energy of interaction of the peptide with the membrane at the configuration was calculated from the electrostatic potential using Eqs. 17–20.
4. Steps 1–3 were repeated for 67 configurations, and the binding constant was calculated by integrating the excess concentration of peptides over distance (Eq. 16).
5. The binding free energy was calculated from the binding constant by the thermodynamic definition (Eq. 4).

Binding constants and binding free energies

We assume that the structure of neither the peptide nor the lipid bilayer changes upon binding. (The role of dynamics is considered, for example, in three recent papers (Zhou and Schulten, 1995; Chiu et al., 1995; Essmann et al., 1995) and is reviewed by Pastor (1994).) Hence the *i*th configuration of the peptide relative to the center of the membrane section, which was chosen as a reference, is uniquely defined by six coordinates: three cartesian coordinates of the location of the geometric center of the peptide x, y, and z; and three angles of rotation and tilts of the peptide around its geometrical center θ, α, and γ. The rotation and tilt angles were measured relative to the orientation depicted in Figs. 2 and 3 (i.e., the peptide parallel to the membrane surface with its backbone in the x direction). Specifically, θ denotes rotations of the peptide around z, the normal to the membrane surface; α denotes rotation of the peptide around x, a virtual axis along the peptide backbone; and γ denotes rotation of the peptide around y, an axis parallel to the membrane surface and perpendicular to the peptide backbone axis (i.e., a tilt with respect to the surface).

The concentration of peptide at R, the minimum distance between the van der Waals surfaces of the peptide and the

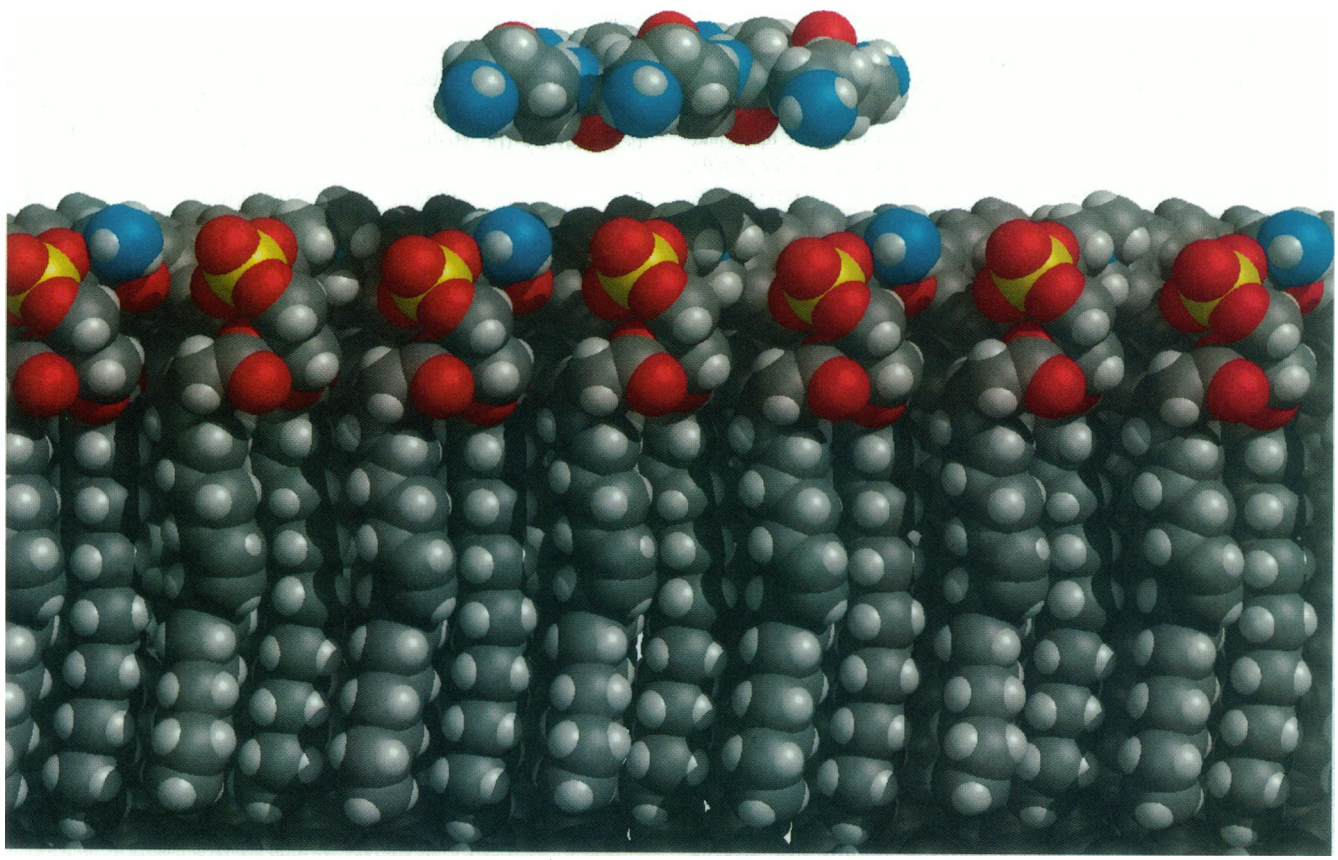

FIGURE 2 Molecular model of a portion of a PC:PS (3:1) bilayer membrane and pentalysine. The PS lipids in the membrane can be recognized by their blue nitrogen atoms. The oxygen atoms are red, the phosphorus atoms yellow, the carbon atoms grey, and the hydrogen atoms white. The membrane is oriented with the normal to its surface along the z axis. The distance between the van der Waals surfaces of the peptide and the membrane in this configuration is R = 2.5 Å.

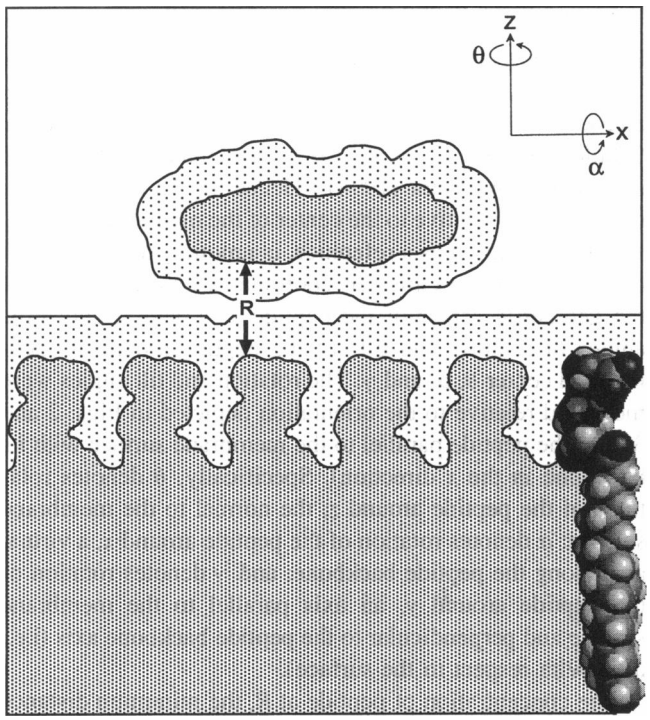

FIGURE 3 A cross section of the membrane-solution interface and pentalysine shown in a configuration similar to that illustrated in Fig. 2. The structure of one PS molecule is shown for reference. The aqueous phase (white region) has a dielectric constant of 80 and contains monovalent salt. The lipids and the peptide (grey regions) have a dielectric constant of 2 and are impenetrable to salt. The ion exclusion layers (stippled regions) have a dielectric constant of 80 and contain no salt; this region extends 2 Å beyond the van der Waals radii of the atoms that constitute the lipids and peptide. R is the distance between the van der Waals surfaces of the peptide and the membrane. The insert illustrates α and θ: two of the angles used to define the orientation of the peptide relative to the x, y, and z axes.

membrane, [P(R)], is proportional to its concentration at infinity, [P_∞], and to the average of the exponent of its free energy of interaction with the membrane (Roth and Lenhoff, (1993):

$$[P(R)] = [P_\infty]\langle\exp(-\beta\Delta W(x, y, R, \theta, \alpha, \gamma))\rangle. \quad (15)$$

Using Eqs. 5, 6, 9, 10, and 15, we obtain the six-dimensional analog of Eq. 11; the binding constant, K, is given as

$$K = CA_L N\int_0^\infty dR\langle\exp[-\beta\Delta W(x, y, R, \alpha, \gamma, \theta)] - 1\rangle. \quad (16)$$

Equation 16 is a more general form of an equation used by Roth and Lenhoff (1993) in their study of the binding of lysozyme to a charged surface. They assumed a simple geometry: a charged sphere interacting with a uniformly charged planar surface. Our Eq. 16 accounts for the exact geometry of both the peptide and the membrane. Sixty-seven different orientations of the peptide (in the 5D space (x, y, β, γ, θ)) were sampled for each R. The convergence with respect to the number of orientations sampled was tested by comparing the values of K obtained using 50 and 67 orientations. The difference of less than 0.2 kcal/mol indicates a sufficient convergence.

The electrostatic free energy of interaction of the peptide and the membrane

The electrostatic free energy of interaction of the peptide with the membrane at the ith configuration, ΔW^i, is defined as the difference between the electrostatic free energy of the system in this configuration, W^i_{p+b}, and the electrostatic free energy when the peptide and the bilayer are infinitely far apart ($W_p + W_b$):

$$\Delta W^i = W^i_{p+b} - (W_p + W_b). \quad (17)$$

The energies W^i_{p+b}, W_p, and W_b were calculated using the nonlinear Poisson-Boltzmann equation (Sharp and Honig, 1990). In calculating the energies we assumed that the ion atmospheres redistribute themselves instantaneously to each configuration of the peptide. The energy is therefore given by

$$\beta W = \int\left(\frac{1}{2}\rho^f(\vec{r})\phi(\vec{r}) - \frac{1}{2}\rho^m(\vec{r})\phi(\vec{r}) - \Delta\pi\right)d\nu, \quad (18)$$

where $d\nu$ is a volume element around a given point, $\vec{r}$, in space. $e\rho^f(\vec{r})$ and $e\rho^m(\vec{r})$ are the charge densities of the fixed and the mobile charges, respectively. Specifically, the fixed charge density includes all of the charges on the membrane and the peptide. The mobile (ionic) charge density in space is given by the Boltzmann relation as

$$\rho^m(\vec{r}) = -2c^b\sinh(\phi(\vec{r})), \quad (19)$$

where c^b is the bulk concentration of (monovalent) ions.

$$\Delta\pi = 2c^b(\cosh(\phi(\vec{r})) - 1) \quad (20)$$

is the excess osmotic pressure contribution to the energy due to the nonuniform distribution of ions in the electric field. Similar calculations have been carried out for salt effects on the binding of ligands and proteins to DNA (Zacharias et al., 1992; Misra et al., 1994a,b).

Note that Eq. 18 reduces to the conventional expression for the electrostatic free energy obtained from the linearized Poisson-Boltzmann equation: $\beta W_{linear} = \frac{1}{2}\int\rho^f(\vec{r})\,\phi(\vec{r})\,d\nu$ for low electrostatic potential (i.e., in the limit of high ionic strength and/or low charge density). The last two terms on the right-hand side of Eq. 18 are the nonlinear contributions to the energy. Their contributions relative to the linear term depend on the ionic strength and the charge. For a 2:1 PC:PS membrane in 100 mM salt, they collectively contribute about 30% of the value of the free energy of interaction.

Model peptides and model membranes

Three (unblocked) basic peptides, Lys_3, Lys_5, and Lys_7, were built in extended form, and energy minimized (2000 iterations of conjugate gradient method) in gas phase using

the CVFF force field (Hagler et al., 1974) in the Insight/Discover molecular modeling package (INSIGHT-II, Biosym Technologies). The minimization did not change the structure significantly; this result is consistent with a strong electrostatic repulsion of the charged lysine residues. The peptides dimensions are 4 Å × 14 Å × 14 Å, 4 Å × 14 Å × 21 Å, and 4 Å × 14 Å × 28 Å, for tri-, penta-, and heptalysine, respectively.

Charged 1-palmitoyl-2-oleoyl-sn-glycero-3-phosphoserine (PS) and neutral 1-palmitoyl-2-oleoyl-sn-glycero-3-phosphocholine (PC) lipids were built using Biograf (Biodesigns, Pasadena, CA) version 2.11 running on an Evans and Sutherland PS 390. These were used to construct model bilayers. Information about the orientation of the polar headgroup and the glycerol backbone comes from NMR (Scherer and Seelig, 1987; Seelig et al., 1987; Smith et al., 1992), neutron and x-ray diffraction (Büldt et al., 1979; Pearson and Pascher, 1979; Hauser et al., 1981; Wiener and White, 1992), and Raman scattering (Akutsu and Nagamori, 1991) measurements. The polar headgroup of our model PC has an ~15° angle of inclination to the bilayer surface, compared to the estimate of ~20° by Wiener and White (1992). The glycerol backbones in our model have an ~25° inclination from the bilayer normal, greater than the ~0° inclination seen for DMPC by x-ray (Pearson and Pasher, 1979) but less than the <~45° inclination deduced for DPPC by NMR (Smith et al., 1992). The structures were energy minimized for 200 cycles using the conjugate gradient method and a Dreiding force field.

Four different lipid bilayers, 1:1, 2:1, 3:1, and 8:1 PC:PS (50%, 33%, 25%, and 11% PS), were built as described by Peitzsch et al. (1995). Each bilayer leaflet contains 192 hexagonally packed lipids, and each lipid has an area of 68 Å^2. The bilayer surface is roughly square, 130 Å × 120 Å, and the bilayers are 60 Å thick. Each leaflet's polar head group region is 7–8 Å thick, which leaves a 45-Å region occupied by the acyl tails. The thickness of the hydrocarbon region agrees with experimental neutron and x-ray diffraction measurements (Wiener and White, 1992). The acidic lipids were distributed on a hexagonal lattice throughout each leaflet, and the leaflets are mirror images of each other. All lipids of the same species were oriented identically in the plane of the membrane. Other researchers have constructed similar molecular models of membranes (reviewed in Stouch, 1993).

The system used in each set of calculations was a combination of one model peptide interacting with one model lipid bilayer. For each calculation, the peptide was placed in a specified position and orientation with respect to the lipid bilayer. For example, Fig. 2 shows Lys_5 oriented parallel to the surface of a 3:1 PC:PS bilayer with approximately 2.5 Å separating their van der Waals surfaces.

Representation on a cubic grid

The method used for representing the peptide and membrane on the lattice has been reviewed by Honig et al. (Honig et al., 1993; Honig and Nicholls, 1995) and was used by Peitzsch et al. (1995) in their study of the electrostatic potential adjacent to membranes. The peptide and the membrane at a given configuration were represented as a set of atomic radii and partial charges, defined at the coordinates of each nucleus. The atoms were mapped onto a cubic grid of l^3 grid points (in most calculations $l = 113$). The charges and radii used for the amino acids were taken from a CHARMM22 parameter set (Brooks et al., 1983), and those used for the lipids are the ones described by Peitzsch et al. (1995).

A smooth molecular surface was generated by rolling a spherical probe with the radius of a water molecule (1.4 Å) over the surface defined by the van der Waals radii of all of the atoms of the peptide and the membrane; the contours traced out by the probe's edge closest to the van der Waals surfaces of the peptide and the membrane atoms were taken as the molecular surfaces. The volume inside the molecular surface (grey regions in Fig. 3) was assigned a dielectric constant of 2, and the outside volume was assigned a value of 80.

The Debye-Hückel parameter, κ, was assigned a value of 0 for all lattice points of zero ionic strength (gray and stippled regions in Fig. 3). A nonzero value of κ (e.g., κ^{-1} = 9.6 Å when the aqueous solution contains 100 mM monovalent ions at 25°C) was assigned to all the other lattice points (white region in Fig. 3). Charges were assigned to the eight lattice points that surround the center of each charged atom using a trilinear interpolation (Klapper et al., 1986).

The electrostatic potential

The Poisson-Boltzmann (PB) equation,

$$\nabla \cdot \epsilon(\vec{r})\nabla\phi(\vec{r}) - \epsilon_r \kappa^2 \sinh(\phi(\vec{r})) + \frac{\beta e^2}{\epsilon_0}\rho^f(\vec{r}) = 0, \quad (21)$$

where $\epsilon(\vec{r})$ is the spatially dependent dielectric constant, was mapped onto a cubic lattice as described above and solved for $\phi(\vec{r})$. The first term in Eq. 21 was represented on the lattice using the finite difference approximation. The quasi-Newton method for treating the nonlinear portion of the PB equation (Holst and Saied, 1993) was combined with three levels of multigridings (Holst, 1993) to solve the equation. The same method was recently used by Peitzsch et al. (1995) in their study of the electrostatic potential adjacent to the model phospholipid bilayer.

In the initial run, a coarse scale of 0.25 grids/Å was used, such that the x dimension of the membrane spanned about 20% of the lattice. At this resolution the electrostatic potential is approximately zero at the grid boundaries. Debye-Hückel potential boundary conditions (Gilson et al., 1988) were used, but the final results did not change significantly when zero or coulombic boundary conditions were applied. A sequence of three focusing runs (Gilson et al., 1988) using finer scales of 0.5, 1.0, and 2.0 grids/Å followed the initial run. The boundary conditions for each of the focusing

runs were taken from the potential calculated in the previous run. Periodic boundary conditions were applied in the x and y axes (the plane of the membrane) for scales of 0.25 and 0.5 grids/Å to mimic an infinite membrane, because the membrane spanned less than 100% of the lattice at these resolutions. At resolutions greater than 0.5 grids/Å, the membrane was larger than the lattice and periodic boundary conditions were not used, to avoid replicating the peptide. Moreover, the periodicity of the membrane is implicitly retained by using the focusing boundary conditions (Peitzsch et al., 1995). Periodic boundary conditions were not used for solving the Poisson-Boltzmann equation for the peptide itself.

Convergence tests

We tested the convergence of the results with respect to the lattice size and scale. Increasing the size of the grid box from 113^3 to either 129^3 or 193^3 points at a constant scale of 2 grids/Å altered the electrostatic free energy of interaction of pentalysine with a 2:1 PC:PS membrane in 100 mM monovalent salt by less than 0.2 kcal/mol. The convergence with respect to lattice scale depended on the distance between the peptide and the membrane and on their relative orientation. The results obtained using a grid box of 129^3 points and scales of 0.5, 1.0, and 2.0 grids/Å differed by less than 0.1 kcal/mol when at least one water molecule fit between the van der Waals surfaces of the membrane and the peptide; the depth of the free energy minimum, which dominates the binding free energy (see Eq. 16), changed by less than 0.2 kcal/mol. We estimate that the free energy of binding deduced from these calculations is accurate to 0.5 kcal/mol.

RESULTS

Experimental measurements

Fig. 4 illustrates the binding of Lys_3, Lys_5, and Lys_7 to vesicles containing 33% acidic phospholipid (2:1 PC:PG vesicles) in 100 mM monovalent salt. The experimental results are described well by Eq. 3; a least-squares fit of this equation to the data gave molar partition coefficients, or apparent association constants of the peptide with a lipid (Eq. 1), of 1.9×10^2, 5.4×10^3, and 1.5×10^5 M^{-1} for Lys_3, Lys_5, and Lys_7, respectively. These correspond to binding free energies of about -3, -5, and -7 kcal/mol for peptides with 3, 5, and 7 basic residues (Eq. 4). Thus each basic residue contributes about -1 kcal/mol binding energy when the membrane contains 33% acidic lipid and the aqueous solutions contains 100 mM KCl. The binding energies deduced from the data in Fig. 4 are plotted as filled circles in Fig. 5 for comparison with the theoretical predictions of two different models. (The data were most accurate for binding energies between 3 and 6 kcal/mol for several technical reasons. We also obtained reliable data for binding energies of about 2 and 7 kcal/mol, although there was more scatter in these experimental measurements, as illustrated by the data for Lys_7 in Fig. 2).

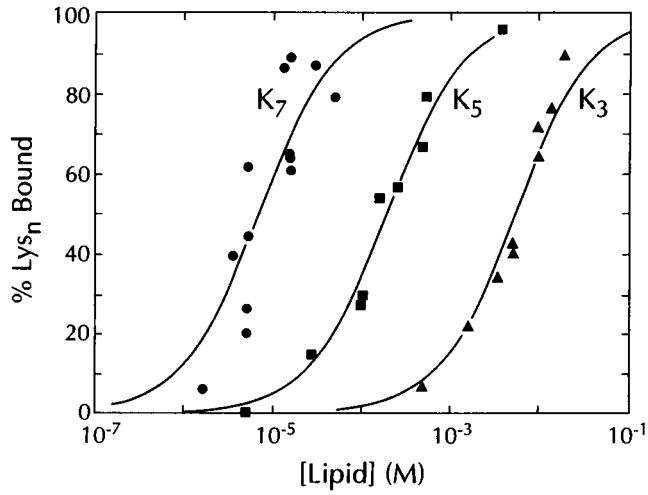

FIGURE 4 Binding of Lys_3, Lys_5, and Lys_7 to large unilamellar vesicles (LUVs). The vesicles were formed from a 2:1 mixture of phosphatidylcholine:phosphatidylglycerol (PC:PG) in 100 mM KCl buffered to pH 7.0 with 1 mM MOPS. The percentage of peptide bound to the vesicles was measured directly by a centrifugation technique. The vesicles were loaded with sucrose to increase their density and centrifuged in the presence of peptides, and the peptide remaining in the supernatant (and in the pellet with the vesicles) was determined using a fluorescamine assay. The curves through the points are the predictions of Eq. 3.

We also measured the binding of Lys_5 to 2:1 PC:PG vesicles in solutions containing 50, 150, 300, or 500 mM

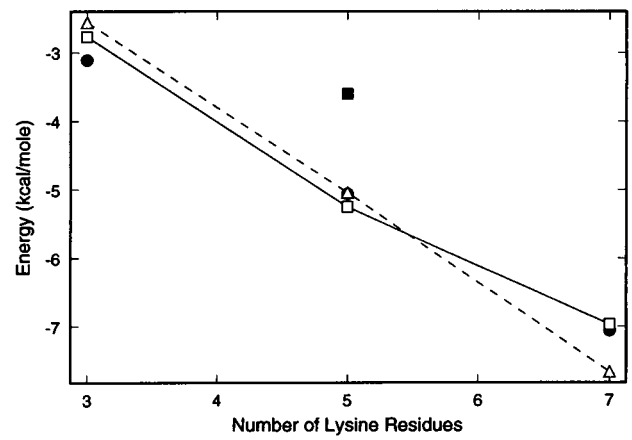

FIGURE 5 Binding energy as a function of the number of lysine residues. The standard Gibbs free energies of binding determined from the experimental data in Fig. 4 are represented as filled circles. The open triangles connected by the dashed line illustrate the predictions of the primitive model, where the membrane is represented as a uniformly charged plane and the peptide is represented as a point charge. The filled square illustrates the prediction of the atomic model. The open squares connected by the solid line illustrate the potential energy of the peptide positioned such that its free energy is minimal as predicted by the atomic model; this orientation and location are illustrated in Fig. 2 for Lys_5. As discussed in the text, this is not the theoretically expected binding energy of the peptide, although the energies fortuitously agree well with the experimental values.

KCl and 1 mM MOPS (pH 7.0). The data at each salt concentration can be described by Eq. 3 about as accurately as the data in Fig. 4. Fig. 6 shows the binding energies determined from these measurements as a function of salt concentration (*filled circles*). Note that increasing the salt concentration from 50 to 500 mM decreases the magnitude of the binding energy from about −7 to −2 kcal/mol. The corresponding reduction in the apparent association constant is from 8×10^4 to 25 M^{-1}.

We also measured the binding of Lys_5 to membranes containing different mole fractions of acidic lipid. The data obtained with 1:1, 4:1, and 9:1 PC:PG membranes can be described by Eq. 3 about as well as the data shown in Fig. 4. Fig. 7 shows the binding energies determined from these measurements as a function of the mol% of acidic lipid in the membranes (*filled circles*). The magnitude of the binding energy increases from about −2 to −6 kcal/mol as the percentage of acidic lipid increases from 10% to 50%. The corresponding increase in the apparent association constant is from about 50 to 3×10^4 M^{-1}. We could not detect any significant binding of pentalysine to PC vesicles using this technique, which implies that the binding energy is <1 kcal/mol.

In summary, the membrane binding energy of these basic peptides increases significantly with an increase in the number of basic residues in the peptide (Fig. 5), a reduction in the ionic strength of the solution (Fig. 6), and an increase in the mol% acidic lipid in the membrane (Fig. 7).

Model 1

Using the model illustrated in Fig. 1 and Eqs. 11–14, we calculated the binding of point charges with valences equal to Lys_3, Lys_5, and Lys_7 with charged slabs. The slabs have charge densities equal to our model phospholipid bilayers. The predictions of this model are shown in Figs. 5, 6, and 7 (*triangles*); the agreement with the experimental results is remarkably good. The model accurately describes not only the dependence of the binding energy on the number of basic residues (Fig. 5), the salt concentration (Fig. 6), and the mol% acidic lipid in the membrane (Fig. 7), but also the absolute value of the binding energy.

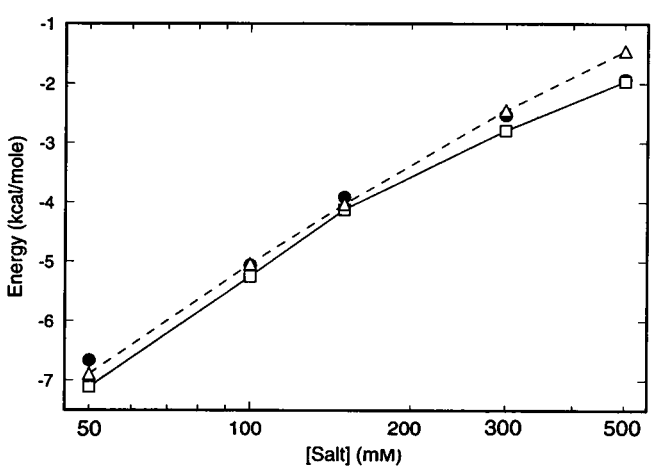

FIGURE 6 Binding energy of pentalysine to bilayers as a function of the salt concentration. The experimentally determined standard Gibbs free energies of binding of pentalysine to 2:1 PC:PG bilayers are represented as filled circles. The open triangles connected by the dashed line illustrate the predictions of the primitive model, where the membrane is represented as a uniformly charged plane and the peptide is represented as a point charge. The open squares connected by the solid line illustrate the potential energy of the peptide in the orientation of Fig. 2 predicted by the atomic model, where its free energy is minimal.

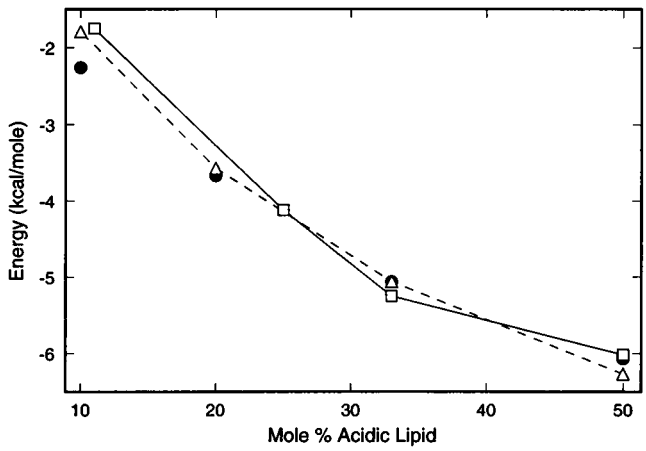

FIGURE 7 Binding energy of pentalysine to bilayers as a function of the mol% of acidic lipid. The experimentally determined standard Gibbs free energies of binding of pentalysine to PC:PG vesicles in 100 mM KCl (plus 1 mM MOPS, pH 7) are represented as filled circles. The open triangles connected by the dashed line illustrate the predictions of the primitive model, where the membrane is represented as a uniformly charged plane and the peptide is represented as a point charge. The open squares connected by the solid line illustrate the potential energy of the peptide in the orientation of Fig. 2 predicted by the atomic model; in this orientation its free energy is minimal.

Model 2: atomic representation

The electrostatic interaction as a function of the peptide-membrane distance

Fig. 8 shows the electrostatic free energy of interaction of pentalysine with a 2:1 PC:PS bilayer in a 100 mM salt solution plotted as a function of the distance R (defined in Fig. 3). The peptide is oriented parallel to the membrane surface as in Fig. 2. This free energy curve illustrates the coulombic attraction between the positively charged peptide and the negatively charged membrane for $R \geq 2.5$ Å (i.e., the minimum distance between the van der Waals surfaces is larger than the 2.8 Å diameter of a water molecule). At shorter distances, however, a portion of the region between the peptide and the membrane (part of the white and stippled regions between pentalysine and the membrane in Fig. 3) is no longer accessible to water and is assigned a low dielectric constant (i.e., "becomes grey" in terms of the scheme in Fig. 3). The charges on the peptide and the membrane in this region are thus transferred to a region of low dielectric constant when pentalysine approaches the

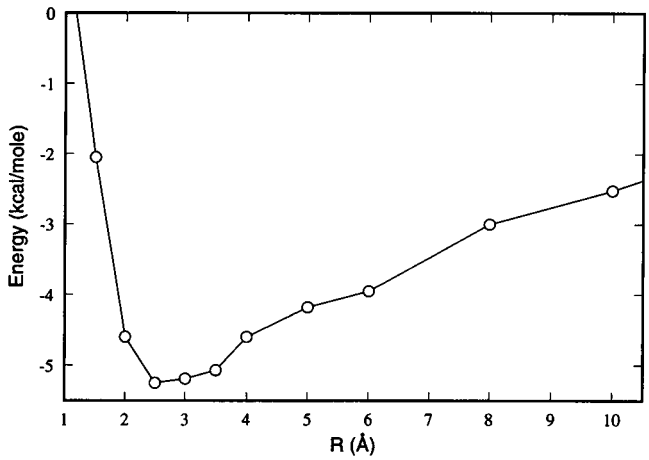

FIGURE 8 Electrostatic free energy curve. The electrostatic free energy of interaction between pentalysine and a 2:1 PC:PS lipid bilayer in 100 mM monovalent salt as a function of the distance R. The peptide is parallel to the membrane surface in the orientation depicted in Fig. 2. A set of charges and radii derived from a CHARMM force field and a probe and ionic radii of 1.4 and 2.0 Å were used. The inner dielectric of the peptide and the membrane was set to 2, and the outer dielectric was set to 80.

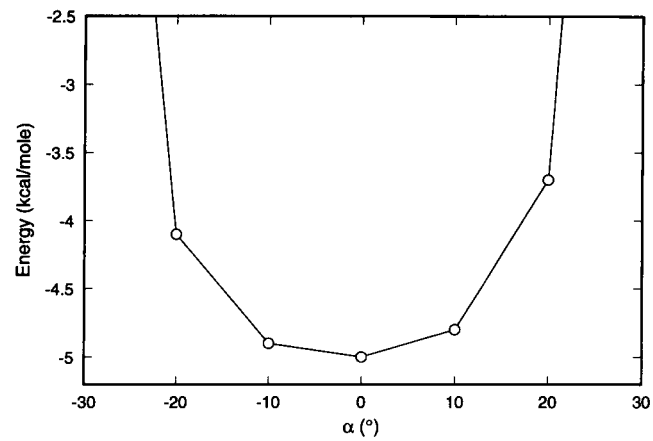

FIGURE 9 Electrostatic free energy of interaction as a function of rotations. The electrostatic free energy of interaction between an acetyl-pentalysine-amide and a 2:1 PC:PS lipid bilayer in 100 mM monovalent salt as a function of rotation of the peptide around the x axis. The axis of the peptide was maintained a constant distance z from the membrane. For $\alpha = 0$ the distance between the peptide and the membrane is $R = 2.5$ Å. A set of charges and radii derived from a CHARMM force field and a probe and ionic radii of 1.4 and 2.0 Å were used, and the inner and outer dielectric constants were set to 2 and 80, respectively.

membrane surface. There is an energy penalty, known as Born repulsion (see, for example, Parsegian, 1969; Andersen, 1978; Torrie et al., 1982), for transferring charges from a high to a low dielectric region. It is clear from the energy curve presented here that the Born repulsion dominates the electrostatic attraction between the oppositely charged peptide and membrane at short distances. (That desolvation forces can dominate over coulombic attractions, leading to apparent repulsion between opposite charges, has been noted in a number of other systems (Parsegian, 1969; Warshel, 1981; Warshel and Schlosser, 1981; Warshel and Russell, 1984; Honig and Hubbell, 1984; Novotny and Sharp, 1992; Zacharias et al., 1992; Hendsch and Tidor, 1994; Tachiya, 1994; Honig and Nicholls, 1995). The physical origin of the phenomenon is discussed in detail in Ben-Tal and Coalson (1994) and Ben-Tal (1995).)

The electrostatic interaction as a function of orientation

Fig. 9 shows how the α rotation of pentalysine around its backbone (see Fig. 3) affects the electrostatic free energy of interaction between the peptide and the bilayer. We used an acetyl-pentalysine-amide to concentrate on effects due to the side chains rather than the charged amino and carboxy termini. If the peptide is close to the membrane surface, the electrostatic free energy minimum occurs when the peptide is parallel to the membrane surface (Fig. 9). Recall that a pentalysine in extended form has a plate-like structure, so that each of its five residues interact equally well with the membrane surface when the peptide is in a parallel orientation. If the peptide is far from the membrane, however, the free energy minimum occurs when the peptide is perpendicular to the membrane because the electrostatic interactions are nonlinear: the energy gained by the proximal residues exceeds the energy lost by the distal residues.

Absolute binding constant

Using Eqs. 16–21, we calculated a binding constant of $\sim 400\ M^{-1}$, which corresponds (via Eq. 4) to a free energy of binding of -3.6 kcal/mol, for pentalysine binding to 2:1 PC:PS bilayer in 100 mM salt. The filled square in Fig. 5 shows the calculated free energy. The calculated binding constant and binding free energy are, respectively, about 10-fold smaller and 1.5 kcal/mol less negative than the measured values, an error of 30%. Explanations for the deviation will be considered in the Discussion.

Calculating the binding constants of the peptides to the membrane requires significant computer time because the Poisson-Boltzmann equation must be solved numerically for the peptide and the membrane in many different configurations. The relative binding free energy (i.e., the dependence of the binding free energy on the number of lysine residues, on the mol% of acidic lipids, and on the ionic strength) is much easier to estimate, however. To a first approximation, we can estimate it from the changes in the depth of the well in the free energy curve that was obtained for Lys_n ($n = 3$, 5, and 7) oriented parallel to the membrane surface (as in Fig. 2). That way, we only needed to calculate a single energy curve of the type shown in Fig. 8 for each set of peptide and membrane at each ionic strength.

Although most of the bound peptides adjacent to the surface of the membrane are in the orientation shown in Fig. 2, some of them are at different distances and/or orientations. As shown by Eq. 16, the binding constant depends primarily on the depth of the energy well of Fig. 8, but it

also depends on its shape. Our approximation, i.e., estimating the relative binding constant based on changes in the depth of this energy well, could lead to errors if the shape also changes. In all of the cases that we studied, the relative binding energy estimated by using the energy at the bottom of the well was the same as the relative binding energy calculated by integration over energy curves such as the one plotted in Fig. 8. For the particular systems studied here, the depth of the well coincides with the experimentally determined standard Gibbs free energy, but this, presumably, is fortuitous.

Dependence of binding on the number of lysine residues

The open squares in Fig. 5 show the value of the electrostatic free energy of interaction at the bottom of the energy well for Lys_3, Lys_5, and Lys_7 oriented parallel to the membrane surface. The membrane contained 2:1 PC:PS, and the salt concentration was 100 mM. In agreement with the trend observed in both the experiments and the primitive model, the binding becomes stronger (i.e., a deeper minimum in the electrostatic free energy curve) as the number of charged residues on the peptide increases. The slope (i.e., the dependence of the calculated binding energy on the number of charged residues) obtained from this model agrees well with the slope observed in the experiments.

Dependence of binding on the ionic strength

The open squares in Fig. 6 show the value of the electrostatic free energy of interaction at the bottom of the energy well for pentalysine oriented parallel to the membrane surface as a function of the ionic strength. The binding gets weaker (i.e., a shallower minimum in the electrostatic free energy curve) as the ionic strength increases. The slope obtained from this model (recall that only the slope is meaningful, as mentioned above) agrees well with the slope of the experimental measurements (*filled circles*).

Dependence of binding on the mol% of acidic lipids

The open squares in Fig. 7 show the value of the electrostatic free energy of interaction at the bottom of the energy well for pentalysine oriented parallel to the membrane surface as a function of the mol% of acidic lipids. The binding becomes stronger as the acidic lipid content of the membrane increases, and once again the slope agrees well with the slope observed in the experiments.

Sensitivity to model parameters

Our calculations used a set of charges and radii derived from CHARMM force field (Brooks et al., 1983) with values for the probe and ionic radii that are traditionally used in continuum models (Honig et al., 1993): a water molecule probe radius of 1.4 Å and an ionic radius of 2.0 Å. We tested the sensitivity of the results to these parameters by using charges and radii sets derived from CHARMM (Brooks et al., 1983), CVFF (Hagler et al., 1974), and PARSE (Sitkoff et al., 1994) and a range of water probes and ionic radii. Some results are presented in Fig. 10.

We varied the probe radius in the range 1.0–1.8 Å and the ionic radius in the range 1.9–2.5 Å and observed deviations of $\leq$0.5 kcal/mol in the energy values. The energy curves obtained using charges and radii derived from CHARMM and CVFF are nearly identical, whereas a somewhat wider and shallower energy minimum is observed using the PARSE parameter set (Fig. 10). A comparison of the energy curves obtained for ionic radii of 2 and 2.2 Å (*circles* and *plus signs*, Fig. 10) shows how the size of the ion exclusion layer (stippled regions in Fig. 3) affects the shape of the energy curve. The salt ions that are located between the peptide and the membrane screen the electrostatic attraction. When the ionic radius is increased, fewer salt ions exist between the peptide and the membrane, the screening is reduced, and the electrostatic attraction increases for $3 < R < 6$ Å, as illustrated in Fig. 10.

Sensitivity to the value of the dielectric constant

Our calculations also used the conventional settings of the dielectric constants: 2 for the interior of the peptide and the membrane, and 80 for the solution (Honig et al., 1993). Whereas there is good experimental evidence that the dielectric constant is 80 for the aqueous phase and 2 for the interior of the membrane, its value in the polar head group

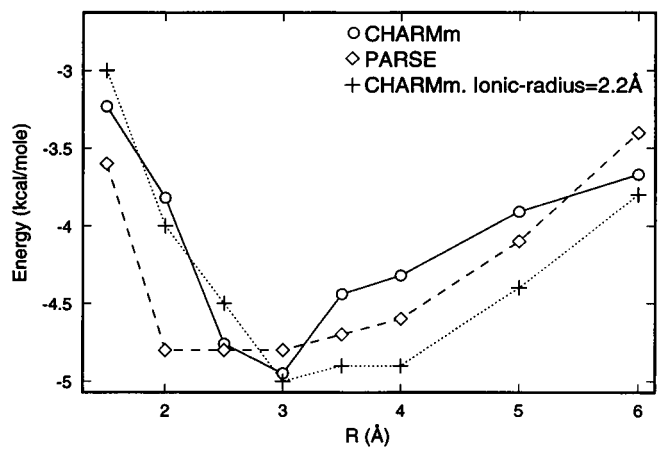

FIGURE 10 Sensitivity to model parameters. The electrostatic free energy of interaction of acetyl-pentalysine-amide with 2:1 PC:PS lipid bilayer in 100 mM monovalent salt as a function of R. The peptide is oriented parallel to the membrane surface as in Fig. 2. The circles connected by the solid line were calculated using the "traditional setting": a charge and radii parameter set derived from CHARMM (Brooks et al., 1983) with ionic and probe radii of 2.0 Å and 1.4 Å, respectively. These parameters are the ones used throughout the paper. The plus signs connected by the dotted line were calculated using the same parameters, but with an ionic radius of 2.2 Å. The diamonds connected by the dashed line were calculated using the PARSE parameter set (Sitkoff et al., 1994) with an ionic radius of 2.0 Å and a probe radius of 1.4 Å. The inner and outer dielectric constants were set to 2 and 80, respectively, throughout this figure.

region is unknown. In the atomic model (see Fig. 3) it can be thought of as a volume-weighted average over its value in the water and in the membrane. We changed the average by changing the value of the dielectric constant of both the inner and the outer regions in the ranges 1–8 and 50–100, respectively. We observed deviations of ≤0.5 kcal/mol from the energy curve obtained for the conventional setting (*circles*, Fig. 11). The one exception is where the interior dielectric is set to 8 (*diamonds*, Fig. 11): the energy well is wider, which would produce a stronger binding constant. Adding an intermediate dielectric region does not alter the electrostatic free energy curve significantly (*plus signs*, Fig. 11).

DISCUSSION

Both electrostatic models we consider describe the experimental data well. Each model predicts reasonably accurately how the binding energy depends on the number of basic residues on the peptide (Fig. 5), the ionic strength of the solution (Fig. 6), and the fraction of acidic lipids in the membrane (Fig. 7). Because the primitive model neglects both the finite size of the peptide and the Born (image charge) effect that repels the peptide from the low dielectric membrane, it must overestimate the concentration of the peptide in the aqueous phase adjacent to the membrane. For a surface equivalent to a 2:1 PC:PS membrane in a 100 mM salt solution, for example, this model predicts that 80% of the pentavalent peptides constituting the Gibbs surface excess (stippled region in Fig. 1 *B*) are located within 1 Å of the surface (see Eq. 8). This is physically unreasonable, given the size of the peptide (Fig. 2). Nevertheless, the model correctly predicts not only the relative but also the absolute values of all of the binding energies we measured (Figs. 5, 6, 7), which implies other attractive nonpolar (e.g., hydrophobic) interactions between the peptide and the membrane may compensate for the Born repulsion. The predictions of the atomic model, which considers the Born repulsion effects and the finite size of the peptide, underestimate the binding energy of pentalysine to a 2:1 PC:PG membrane by about 1.5 kcal/mol (Fig. 5, *filled square*). This also implies that the model ignores some attractive interactions.

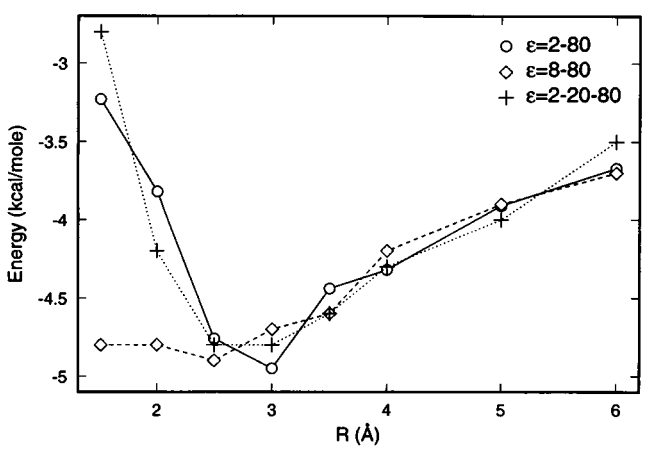

FIGURE 11 Sensitivity to the value of the dielectric constant. The electrostatic free energy of interaction of acetyl-pentalysine-amide with 2:1 PC:PS lipid bilayer in 100 mM monovalent salt as a function of the distance *R*. The peptide is oriented parallel to the membrane surface as in Fig. 2. The circles connected by the solid line were calculated using the traditional setting: inner and outer dielectric constants of 2 and 80, respectively. These values are the ones used throughout the paper. The diamonds connected by the dashed line were calculated using inner and outer dielectric constants of 8 and 80, respectively. The plus signs connected by the dotted line were calculated for three dielectric regions: the inner dielectric was 2, the outer dielectric was 80, and the ion exclusion layer (the stippled regions of Fig. 3) was assigned a dielectric of 20. Atomic radii and charges derived from CHARMM (Brooks et al., 1983) with ionic and probe radii of 2.0 and 1.4 Å, respectively, were used throughout the figure.

The attractive nonpolar interactions can be estimated by assuming that they are proportional to the water-accessible surface area (Nozaki and Tanford, 1971; Hermann, 1972; Chothia, 1976; Sitkoff et al., 1994). This area decreases when the distance between the peptide and the membrane, *R* in Fig. 3, becomes less than the diameter of a water molecule. We estimated these nonpolar interactions at each configuration from the reduction in the water-accessible surface area using a surface tension coefficient of 28 cal/mol/Å^2 (Sitkoff et al., 1996). These calculations suggest that nonpolar contributions could add about 1 kcal/mol to the calculated free energy of binding. Thus they could account for the small (1.5 kcal/mol) discrepancy between the predictions of the atomic model and the experimental results.

In addition to ignoring nonelectrostatic contributions to the binding energy, our atomic model ignores or oversimplifies other important factors. For example, we consider only a static model of a peptide and a membrane and ignore any structural changes that may occur as they approach each other. Specifically, the orientation of both the lipid headgroups and the side chains of the amino acids, particularly the charged ones, may change. (Recall that we did sample a number of orientations of the peptide with respect to the membrane in the atomic model calculations, which may approximate a complete Monte Carlo sampling over different structures.) We further investigated the importance of peptide flexibility by studying the membrane binding of charybdotoxin and its analogs, small basic peptides with a rigid structure due to three disulfide bonds (Bontems et al., 1992). The radioactively labeled charybdotoxin we used (valence = 4) binds to phospholipid vesicles (formed at different salt concentrations with different mole fractions of acidic lipids) with about the same association constant as the comparably charged flexible peptides studied here (⟨pentalysine⟩, trilysine), which suggests that peptide flexibility does not play a large role in determining the membrane binding energy of a hydrophilic basic peptide (Ben-Tal et al., manuscript in preparation). Our model also ignores both membrane undulations and the bobbing motions of lipids (McIntoch and Simon, 1994) discussed in recent dynamical studies (Zhou and Schulten, 1995; Chiu et al., 1995). One experiment suggests that these motions do

not significantly affect the binding of basic peptides: pentalysine binds with the same energy to membranes in the liquid-crystalline and in the gel states (Kim et al., 1991).

Finally, our model assumes a sharp, discontinuous boundary between the membrane and the aqueous phase. The membrane surface, however, is "soft," and the polar headgroups may rearrange themselves to minimize the "Born repulsion" by exposing a portion of their charge to the aqueous phase, even when the peptide is close to the surface. Although the continuum model used in this work is extremely accurate in its treatment of solvation phenomena in the bulk aqueous phase (Sitkoff et al., 1994, 1996; Honig and Nicholls, 1995), the ambiguity in defining the membrane/water interface adds a degree of uncertainty to our results. To test their sensitivity to our treatment of solvation, we reduced the radius of the water probe from its standard value of 1.4 Å to 0.5 Å, which has the effect of reducing the Born repulsion. The resulting energy curve was deeper and wider and the free energy of binding calculated using the smaller probe is about 1 kcal/mol more negative. The Born repulsion also depends on the value of the dielectric constant assigned to the polar headgroups. Although direct experimental measurements show the dielectric constant of the membrane interior is 2, both experimental (Ashcroft et al., 1981) and theoretical (Zhou and Schulten, 1995) studies suggest the dielectric is >2 in the headgroup. Assigning a more appropriate dielectric constant to the polar headgroup reduces the Born repulsion, producing a wider free energy well. We can estimate the magnitude of the effect by comparing the free energy curves calculated using inner dielectric constants of 2 and 8 (Fig. 11): indeed, a wider energy well (which implies stronger binding) was predicted using the higher dielectric.

The electrostatic free energies of peptide-membrane interaction calculated here are significantly less negative than those calculated by Roush et al. (1994) in their study of protein-surface interactions. One difference between the two models is that they used the linearized, rather than the nonlinearized, Poisson-Boltzmann equation, but that cannot account fully for the large energy gap between their calculations and ours. Our results are in better agreement with those of Lenhoff and co-workers, who studied the interactions of enzymes with a negatively charged surface (Yoon and Lenhoff, 1992; Roth and Lenhoff, 1993).

Our observation that each basic residue contributes about 1 kcal/mol to the membrane binding energy under physiological conditions (Fig. 5) is directly relevant to understanding how a number of important proteins bind to membranes. Binding of the myristoylated proteins Src (Resh, 1993, 1994) and MARCKS (Aderem, 1992; Blackshear, 1993) to the plasma membrane, for example, requires both the hydrophobic insertion of the myristate chain into the hydrocarbon interior of the membrane and the electrostatic interaction of a cluster of basic residues with acidic lipids (McLaughlin and Aderem, 1995). A (nonmyristoylated) peptide corresponding to the cluster of basic residues on Src (residues 2–16) has a valence of about +5 and binds to membranes containing acidic lipids with the same affinity as pentalysine (Buser et al., 1995). The cluster of basic residues on MARCKS begins with five lysine residues, and the basic membrane binding region of the farnesylated protein K-ras (Hancock et al., 1990; Cadwallader et al., 1994) contains six contiguous lysine residues.

Thus, the work we describe here is directly relevant to the membrane binding of these myristoylated and farnesylated proteins and should help us understand, from first principles, two biologically significant phenomena. First, PKC phosphorylation of serine residues within the cluster of basic residues on MARCKS causes the intact protein (or peptides that correspond to this cluster) to translocate from the membrane to the cytoplasm (or solution), presumably by a simple electrostatic mechanism (McLaughlin and Aderem, 1995). Second, MARCKS exists in a punctuate distribution in the plasma membrane of macrophages and other cells (Rosen et al., 1990). Yang and Glaser (1995) showed that a peptide corresponding to the basic region, MARCKS(151–175) spontaneously forms lateral domains enriched in the acidic lipid PS in phospholipid vesicles. Pentalysine also forms lateral domains enriched in the acidic lipid PS (Denisov et al., 1996). The domains formed in phospholipid vesicles by basic peptides must represent a minimum free energy state that can be examined theoretically with the atomic model described here. Furthermore, these domains may be important for a number of signal transduction events. For example, the acidic lipid PIP_2 is sequestered with PS in these domains. Thus the MARCKS(151–175) peptide and pentalysine inhibit the action of phosphoinositide-specific phospholipases (PLCs) that hydrolyze PIP_2 and produce the two second messengers inositol trisphosphate and diacylglycerol (unpublished data).

Many other proteins use electrostatic interactions to bind to biological membranes. As the structures of these proteins are revealed (e.g., the HIV matrix protein (Zhou et al., 1994; Massiah et al., 1994), cytochrome *c* (Heimburg and Marsh, 1995) or the C2 membrane binding region of proteins such as PKC (Sütton et al., 1995; Newton, 1995)), it should be possible to examine theoretically the interaction of these proteins with acidic phospholipids in membranes.

We thank Carey Bagdassarian, Avinoam Ben-Shaul, Adrian Parsegian, Kim Sharp, Dirk Stigter, and Stephen White for helpful discussions.

BH acknowledges the support of NSF grant MCB-9304127, the National Center for Research Resources division of the Biomedical Technology Program at the NIH, through a Research Resource grant (P41 RR06892) at Columbia University. SM acknowledges the support of NSF grant MCB-9419175, NIH grant GM24971, and American Cancer Society grant PF-3907 to RMP. The calculations were carried out on the CM-5 platforms at Columbia University and the National Center for Supercomputing Applications (University of Illinois at Urbana-Champaign) under grant MCB94000SN, on the CONVEX at Frederick Biomedical Supercomputing Center (FBSC) at the Frederick Cancer Research and Development Center, and on the Power Challenge at the National Center for Supercomputing Applications (University of Illinois at Urbana-Champaign under grant MCA95C01SP).

REFERENCES

Aderem, A. 1992. The MARCKS brothers: a family of protein kinase c substrates. *Cell.* 71:713–716.

Akutsu, H., and T. Nagamori. 1991. Conformational analysis of the polar head group in phosphatidylcholine bilayer: a structural change induced by cations. *Biochemistry.* 30:4510–4516.

Andersen, O. S. 1978. Permeability properties of unmodified lipid bilayer membranes. *In* Membrane Transport in Biology, Vol. 1. G. Giebisch, D. C. Tosteson, and H. H. Ussing, editors. Springer, New York. 371–446.

Ashcroft, R. G., H. G. L. Coster, and J. R. Smith. 1981. The molecular organization of biomolecular lipid membranes. The dielectric structure of the hydrophilic/hydrophobic interface. *Biochim. Biophys. Acta.* 643: 191–204.

Aveyard, R., and D. A. Haydon. 1973. Introduction to the Principles of Surface Chemistry. Cambridge: Cambridge University Press.

Ben-Tal, N. 1995. The energetics of colloids: do oppositely charged particles necessary attract each other? *J. Phys. Chem.* 99:9642–9645.

Ben-Tal, N., and R. D. Coalson. 1994. Dielectric constant effects on the energetics of oppositely charged colloids: a lattice field theory study. *J. Chem. Phys.* 101:5148–5166.

Blackshear, P. J. 1993. The MARCKS family of cellular protein kinase c substrates. *J. Biol. Chem.* 268:1501–1504.

Bockris, J. O'M., and S. U. M. Khan. 1993. Surface Electrochemistry. Plenum, New York, and Rosetta edition. 63–64.

Boguslavsky, V., M. Rebecchi, A. J. Morris, D.-Y. Jhon, S. G. Rhee, and S. McLaughlin. 1994. Effect of monolayer surface pressure on the activities of phosphoinositide-specific phospholipase c-β_1, -γ_1, and -δ_1. *Biochemistry.* 33:3032–3037.

Bontems, F., B. Gilquin, C. Roumestand, A. Menez, and F. Toma. 1992. Analysis of side-chain organization on a refined model of charybdotoxin: structural and functional implications. *Biochemistry.* 31: 7756–7764.

Brooks, B. R., R. E. Bruccoleri, B. D. Olafson, D. J. States, S. Swaminathan, and M. Karplus. 1983. CHARMM: a program for macromolecular energy, minimization, and dynamics calculations. *J. Comput. Chem.* 4:187–217.

Büldt, G., H. U. Gally, A. Seelig, and G. Zaccai. 1979. Neutron diffraction studies on phosphatidylcholine model membrane. I. Head group conformation. *J. Mol. Biol.* 134:673–691.

Buser, C. A., J. Kim, S. McLaughlin, and R. M. Peitzsch. 1995. Does the binding of clusters of basic residues to acidic lipids induce domain formation in membranes? *Mol. Membr. Biol.* 12:69–75.

Buser, C. A., C. T. Sigal, M. D. Resh, and S. McLaughlin. 1994. Membrane binding of myristoylated peptides corresponding to the NH2 terminus of Src. *Biochemistry.* 33:13093–13101.

Cadwallader, K. A., H. Paterson, S. G. Macdonald, and J. F. Hancock. 1994. N-terminally myristoylated Ras proteins require palmitoylation or a polybasic domain for plasma membrane localization. *Mol. Cell. Biol.* 14:4722–4730.

Chiu, S.-W., M. Clark, V. Balaji, S. Subramaniam, H. L. Scott, and E. Jakobsson. 1995. Incorporation of surface tension into molecular dynamics simulations of an interface: a fluid phase lipid bilayer membrane. *Biophys. J.* 69:1230–1245.

Chothia, C. 1976. The nature of the accessible and buried surface in proteins. *J. Mol. Biol.* 105:1–14.

Davis, M. E., and J. A. McCammon. 1990. Electrostatics in biomolecular structure and dynamics. *Chem. Rev.* 90:509–521.

de Kroon, A. I., J. A. Killian, J. de Gier, and B. de Kruijf. 1991. The membrane interaction of amphiphilic model peptides affects phosphatidylserine headgroup and acyl chain order and dynamics. Application of the "phospholipid headgroup electrometer" concept to phosphatidylserine. *Biochemistry.* 30:1155–1162.

de Kroon, A. I., M. W. Soekarjo, J. de Gier, and B. de Kruijff. 1990. The role of charge and hydrophobicity in peptide-lipid interaction: a comparative study based on tryptophan fluorescence measurements combined with the use of aqueous and hydrophobic quenchers. *Biochemistry.* 29:8229–8240.

de Kruijff, B., A. Rietveld, N. Telders, and B. Vaandrager. 1985. Molecular aspects of the bilayer stabilization induced by poly(L-lysines) of varying size in cardiolipin liposomes. *Biochim. Biophys. Acta.* 820: 295–304.

Denisov, G., S. Wanaski, L. Peng, M. Glaser, and S. McLaughlin. 1996. Domain formation induced by binding of basic ligands to membranes containing acidic lipids: an electrostatic mechanism. *Biophys. J.* 70: A223.

Dufourcq, J., J. F. Faucon, R. Maget-Dana, M. P. Pileni, and C. Hélène. 1981. A fluorescence study of the binding of oligopeptides containing aromatic and basic residues to phospholipids vesicles. *Biochim. Biophys. Acta.* 649:67–75.

Essmann, U., L. Perera, and M. L. Berkowitz. 1995. On the origin of the hydration interaction of lipid bilayers from MD simulation of DPPC membranes in gel and liquid crystalline phases. *Langmuir.* 11: 4519–4534.

Fromherz, P. 1975. Instrumentation for handling monomolecular films at an air-water interface. *Rev. Sci. Instrum.* 46:1380–1385.

Gilson, M., K. A. Sharp, and B. Honig. 1988. Calculating the electrostatic potential of molecules in solution: method and error assessment. *J. Comp. Chem.* 9:327–335.

Hagler, A. T., E. Huler, and S. Lifson. 1974. Energy functions for peptides and proteins. I. Derivation of a consistent force field including the hydrogen bond from amide crystals. *J. Am. Chem. Soc.* 96:5319–5327.

Hancock, J. F., H. Paterson, and C. J. Marshall. 1990. A polybasic domain or palmitoylation is required in addition to the CAAX motif to localize p21ras to the plasma membrane. *Cell.* 63:133–139.

Hauser, H., I. Pascher, R. H. Pearson, and S. Sundell. 1981. Preferred conformation and molecular packing of phosphatidylethanolamine and phosphatidylcholine. *Biochim. Biophys. Acta.* 650:21–51.

Heimburg, T., and D. Marsh. 1995. Protein surface-distribution and protein-protein interactions in the binding of peripheral proteins to charged lipid membranes. *Biophys. J.* 68:5436–5546.

Hendsch, Z. S., and B. Tidor. 1994. Do salt bridges stabilize proteins? A continuum electrostatic analysis. *Protein Sci.* 3:211–226.

Hermann, R. B. 1972. Theory of hydrophobic bonding. II. The correlation of hydrocarbon solubility in water with solvent cavity area. *J. Phys. Chem.* 76:2754–2759.

Holst, M. 1993. Numerical solutions to the finite difference Poisson-Boltzmann equation. PhD thesis. University of Illinois, Urbana, IL.

Holst, M., and F. Saied. 1993. Numerical solutions of the Poisson-Boltzmann equation. *J. Comp. Chem.* 14:105–113.

Honig, B. H., and W. L. Hubbell. 1984. Stability of "salt bridges" in membrane proteins. *Proc. Natl. Acad. Sci. USA.* 81:5412–5416.

Honig, B., and A. Nicholls. 1995. Classical electrostatics in biology and chemistry. *Science.* 268:1144–1149.

Honig, B., K. Sharp, and A.-S. Yang. 1993. Macroscopic models of aqueous solutions: biological and chemical applications. *J. Phys. Chem.* 97:1101–1109.

Hope, M. J., M. B. Bally, G. Webb, and P. R. Cullis. 1985. Production of large unilamellar vesicles by a rapid extrusion procedure. Characterization of size distribution, trapped volume and ability to maintain a membrane potential. *Biochim. Biophys. Acta.* 812:55–65.

Israelachvili, J. N. 1992. Intermolecular and Surface Forces. Academic, New York.

Israelachvili, J. N., and H. Wennerström. 1996. Role of hydration and water structure in biological and colloidal interactions. *Nature.* 379: 219–225.

Kim, J., P. J. Blackshear, J. D. Johnson, and S. McLaughlin. 1994. Phosphorylation reverses the membrane association of peptides that correspond to the basic domains of MARCKS and neuromodulin. *Biophys. J.* 67:227–237.

Kim, J., M. Mosior, L. A. Chung, H. Wu, and S. McLaughlin. 1991. Binding of peptides with basic residues to membranes containing acidic phospholipids. *Biophys. J.* 60:135–148.

Klapper, I., R. Hagstrom, R. Fine, K. Sharp, and B. Honig. 1986. Focusing of electrostatic fields in the active site of Cu-Zn superoxide dismutase: effects of ionic strength and amino-acid modification. *Proteins.* 1:47–59.

Massiah, M. A., M. R. Starich, C. Paschall, M. F. Summers, A. M. Christensen, and W. I. Sundquist. 1994. Three-dimensional structure of the human immunodeficiency virus type 1 matrix protein. *J. Mol. Biol.* 244:198–223.

McIntoch, T. J., and S. A. Simon. 1994. Hydration and steric pressures between phospholipid bilayers. *Annu. Rev. Biophys. Biomol. Struct.* 23:27–51.

McLaughlin, S. 1989. The electrostatic properties of membranes. *Annu. Rev. Biophys. Biophys. Chem.* 18:113–136.

McLaughlin, S., and A. Aderem. 1995. The myristoyl-electrostatic switch: a modulator of reversible protein-membrane interactions. *Trends Biochem. Sci.* 20:272–276.

Misra, V. K., J. L. Hecht, K. A. Sharp, R. A. Friedman, and B. Honig. 1994a. Salt effect on protein-DNA interactions: the λcI repressor and *Eco*RI endonuclease. *J. Mol. Biol.* 238:264–280.

Misra, V. K., K. A. Sharp, R. A. Friedman, and B. Honig. 1994b. Salt effect on ligand-DNA binding: minor groove binding antibiotics. *J. Mol. Biol.* 238:245–263.

Montich, G., S. Scarlata, S. McLaughlin, R. Lehrmann, and J. Seelig. 1993. Thermodynamic characterization of the association of small basic peptides with membranes containing acidic lipids. *Biochim. Biophys. Acta.* 1146:17–24.

Mosior, M., and S. McLaughlin. 1992a. Binding of basic peptides to acidic lipids in membranes: effects of inserting alanine(s) between the basic residues. *Biochemistry.* 31:1767–1773.

Mosior, M., and S. McLaughlin. 1992b. Electrostatics and reduction of dimensionality produce apparent cooperativity when peptides bind to acidic lipids in membranes. *Biochim. Biophys. Acta.* 1105:185–187.

Mui, B. L.-S., P. R. Cullis, E. A. Evans, and T. D. Madden. 1993. Osmotic properties of large unilamellar vesicles prepared by extrusion. *Biophys. J.* 64:443–453.

Newton, A. C. 1995. Seeing two domains. *Curr. Biol.* 5:973–976.

Novotny, J., and K. Sharp. 1992. Electrostatic fields in antibodies and antibody/antigen complexes. *Prog. Biophys. Mol. Biol.* 58:203–224.

Nozaki, Y., and C. H. Tanford. 1971. The solubility of amino acids and two glycine peptides in aqueous ethanol and dioxane solutions. Establishment of a hydrophobicity scale. *J. Biol. Chem.* 246:2211–2217.

Parsegian, A. 1969. Energy of ion crossing a low dielectric membrane: solution to four relevant electrostatic problems. *Nature.* 221:844–846.

Pastor, R. W. 1994. Molecular dynamics and monte carlo simulations of lipid bilayers. *Curr. Opin. Struct. Biol.* 4:486–492.

Pearson, R. H., and I. Pascher. 1979. The molecular structure of lecithin dihydrate. *Nature.* 281:499–501.

Peitzsch, R. M., M. Eisenberg, K. A. Sharp, and S. McLaughlin. 1995. Calculations of the electrostatic potential adjacent to model phospholipid bilayers. *Biophys. J.* 68:729–738.

Peitzsch, R. M., and S. McLaughlin. 1993. Binding of acylated peptides and fatty acids to phospholipid vesicles: pertinence to myristoylated proteins. *Biochemistry.* 32:10436–10443.

Rebecchi, M. J., A. A. Peterson, and S. McLaughlin. 1992. Phosphoinositide-specific phospholipase C-delta 1 binds with high affinity to phospholipid vesicles containing phosphatidylinositol 4,5-bisphosphate. *Biochemistry.* 31:12742–12747.

Resh, M. D. 1993. Interaction of tyrosine kinase oncoproteins with cellular membranes. *Biochim. Biophys. Acta.* 1155:307–322.

Resh, M. D. 1994. Myristylation and palmitylation of Src family members: the fats of the matter. *Cell.* 76:411–413.

Rosen, A., K. F. Keenan, M. Thelen, A. C. Nairn, and A. Aderem. 1990. Activation of protein kinase C results in the displacement of its myristoylated, alanine-rich substrate from punctate structures in macrophage filopodia. *J. Exp. Med.* 172:1211–1215.

Roth, C. M., and A. M. Lenhoff. 1993. Electrostatic and van der Waals contributions to protein adsorption: computation of equilibrium constants. *Langmuir.* 9:962–972.

Roush, D. J., D. S. Gill, and R. C. Willson. 1994. Electrostatic potentials and electrostatic interaction energies of rat cytochrome b5 and a simulated anion-exchange adsorbent surface. *Biophys. J.* 66:1290–1300.

Roux, M., J. M. Neumann, M. Bloom, and P. F. Devaux. 1988. ^{2}H and ^{31}P NMR study of pentalysine interaction with headgroup deuterated phosphatidylcholine and phosphatidylserine. *Eur. Biophys. J.* 16:267–273.

Scherer, P. G., and J. Seelig. 1987. Structure and dynamics of the phosphatidylcholine and the phosphatidylethanoamine head group in L-M fibroblasts as studied by deuterium nuclear magnetic resonance. *EMBO J.* 6:2915–2922.

Seelig, A. 1987. Local anesthetics and pressure: a comparison of dibucaine binding to lipid monolayers and bilayers. *Biochim. Biophys. Acta.* 899: 196–204.

Seelig, A. 1992. Interaction of a substance P agonist and of substance P antagonists with lipid membranes. A thermodynamic analysis. *Biochemistry.* 31:2897–2904.

Seelig, J., P. M. Macdonald, and P. G. Scherer. 1987. Phospholipid head groups as sensors of electrostatic charge in membranes. *Biochemistry.* 26:7535–7541.

Sharp, K. A. 1994. Electrostatic interactions in macromolecules. *Curr. Opin. Struct. Biol.* 4:234–239.

Sharp, K. A., and B. Honig. 1990. Calculating total electrostatic energies with the nonlinear Poisson-Boltzmann equation. *J. Phys. Chem.* 94: 7684–7692.

Sigal, C. T., W. Zhou, C. A. Buser, S. McLaughlin, and M. D. Resh. 1994. Amino-terminal basic residues of Src mediate membrane binding through electrostatic interaction with acidic phospholipids. *Proc. Natl. Acad. Sci. USA.* 91:12253–12257.

Sitkoff, D., N. Ben-Tal, and B. Honig. 1996. Calculation of alkane to water solvation free energies using continuum solvent models. *J. Phys. Chem.* 100:2744–2752.

Sitkoff, D., K. Sharp, and B. Honig. 1994. Accurate calculations of hydration free energies using macroscopic solvent models. *J. Phys. Chem.* 98:1978–1988.

Smith, S. O., I. Kustanovich, S. Bhamidipati, A. Salmon, and J. A. Hamilton. 1992. Interfacial conformation of dipalmitoylglycerol and dipalmitoylphosphatidylcholine in phospholipid bilayers. *Biochemistry.* 31:11660–11664.

Stouch, T. R. 1993. Lipid membrane structure and dynamics studies by all-atom molecular dynamics simulations of hydrated phospholipid bilayers. *J. Mol. Simulations.* 10:335–362.

Sütton, R. B., B. A. Davletov, A. M. Berghuis, T. C. Sudof, and S. R. Sprang. 1995. Structure of the first C2 domain of synaptotagmin I: a novel Ca2+/phospholipid-binding fold. *Cell.* 80:929–938.

Tachiya, M. 1994. Energetics of electron transfer reaction in polar solvents. *Chem. Phys. Lett.* 230:491–494.

Tamm, L. K. 1991. Membrane insertion and lateral mobility of synthetic amphiphilic signal peptides in lipid model membranes. *Biochim. Biophys. Acta.* 1071:123–148.

Thorgeirsson, T. E., Y. G. Yu, and Y.-K. Shin. 1995. A limiting law for the electrostatics of the binding of polypeptides to phospholipid bilayers. *Biochemistry.* 34:5518–5522.

Torrie, G. M., J. P. Valleau, and G. N. Patey. 1982. Electrical double layer. II. Monte Carlo and HNC studies of image effects. *J. Chem. Phys.* 76:4615–4622.

Warshel, A. 1981. Electrostatic basis of structure-function correlation in proteins. *Acc. Chem. Res.* 14:284–290.

Warshel, A., and S. T. Russell. 1984. Calculations of electrostatic interactions in biological systems and in solutions. *Q. Rev. Biophys.* 17:283–422.

Warshel, A., and D. W. Schlosser. 1981. Electrostatic control of the efficiency of light-induced electron transfer across membranes. *Proc. Natl. Acad. Sci. USA.* 78:5564–5568.

Wiener, M. C., and S. H. White. 1992. Structure of a fluid dioleoylphosphatidylcholine bilayer determined by joint refinement of x-ray and neutron diffraction data. III. Complete structure. *Biophys. J.* 61:434–447.

Yang, L., and M. Glaser. 1995. Membrane domains containing phosphatidylserine and substrate can be important for the activation of protein kinase C. *Biochemistry.* 34:1500–1506.

Yoon, B. J., and A. M. Lenhoff. 1992. Computation of the electrostatic interaction energy between a protein and a charged surface. *J. Phys. Chem.* 96:3130–3134.

Zacharias, M., B. A. Luty, M. E. Davis, and J. A. McCammon. 1992. Poisson-Boltzmann analysis of the lambda repressor-operator interaction. *Biophys. J.* 63:1280–1285.

Zhou, F., and K. Schulten. 1995. Molecular dynamics study of a membrane-water interface. *J. Phys. Chem.* 99:2195–2207.

Zhou, W., L. J. Parent, J. W. Wills, and M. D. Resh. 1994. Identification of a membrane-binding domain within the amino-terminal region of human immunodeficiency virus type 1 Gag protein which interacts with acidic phospholipids. *J. Virol.* 68:2556–2569.